

Online Supplemental Material

Adipocyte glucocorticoid receptor activation with high glucocorticoid doses impairs healthy adipose tissue expansion by repressing angiogenesis

Anna Vali^{1,2}, Héloïse Dalle^{1,2§}, Alya Loubaresse^{1,2§}, Jérôme Gilleron³, Emmanuelle Havis⁴, Marie Garcia^{1,2}, Carine Beaupère^{1,2}, Clémentine Denis^{1,2}, Natacha Roblot^{1,2}, Karine Poussin^{1,2}, Tatiana Ledent¹, Benjamin Bouillet^{1,2}, Mireille Cormont³, Jean-François Tanti³, Jacqueline Capeau^{1,2}, Camille Vazier^{1,2,5}, Bruno Fève^{1,2,5*}, Alexandra Grosfeld^{1,2*}, Marthe Moldes^{1,2#}

Affiliations

¹Sorbonne Université, Inserm, Centre de Recherche Saint-Antoine, CRSA, F-75012 Paris, France

²Sorbonne Université, Inserm, Institute of CardioMetabolism and Nutrition, ICAN, F-75013 Paris, France

³Université Côte d'Azur, Inserm, C3M, Team Cellular and Molecular Pathophysiology of Obesity, Nice, France

⁴Sorbonne Université, CNRS, Inserm, Laboratoire de Biologie du Développement, Institut Biologie Paris Seine, IBPS, F75005 Paris, France

⁵Sorbonne Université, Inserm, Centre de Recherche Saint-Antoine, CRSA, AP-HP, Hôpital Saint-Antoine, Service Endocrinologie, CRM PRISIS, 75012 Paris, France

* and §these authors contributed equally.

#Correspondence should be addressed to marthe.moldes@inserm.fr

Supplemental Methods

Animals and treatments

All animals were housed with a 12 h light/dark cycle and had free access to water and standard chow diet (LASQCdiet® Rod16-R, LASvendi, Soest, Germany). Body mass composition was measured using an EchoMRI 100 Whole Body Composition Analyzer (EchoMRI, Houston, TX) according to the manufacturer's instructions.

Cell culture

3T3-F442A preadipocytes were maintained in DMEM high glucose (ThermoFisher Scientific, Montigny-le-Bretonneux, France) with penicillin (100 U/mL) and streptomycin (100 µg/mL) (Sigma–Aldrich, Saint Quentin Fallavier; France) supplemented with 10% bovine calf serum (Dutscher, Issy-les-Moulineaux, France) at 37°C in a 5% CO₂ humidified atmosphere. Differentiation was induced in DMEM supplemented with 10% fetal calf serum (FCS, Dutscher) and 1 µM of bovine insulin (Sigma-Aldrich) renewed every other day until total differentiation (day 10). The day before the experiment, mature adipocytes were starved in dexamethasone- and insulin-free DMEM supplemented with 0.1 % BSA (bovine serum albumin, Sigma-Aldrich) for 24 h prior to dexamethasone treatment.

RNA extraction and RT-qPCR analysis

Total RNA from human and murine tissues and adipocyte / SVF fractions were purified by Qiazol extraction and purification using Qiagen RNeasy minicolumns according to the manufacturer's instructions (Qiagen, Courtaboeuf, France). 3T3-F442A adipocytes were directly lysed in RLT buffer of Qiagen RNeasy minicolumns kit as recommended by manufacturer (Qiagen). One µg of total RNA was reverse-transcribed using the High Capacity cDNA Reverse Transcription kit (Applied Biosystems, Foster City, CA, USA). cDNA was

amplified using specific primers and the SYBR Green PCR Master mix (Applied Biosystems) according to manufacturer's instructions, using a QuantStudio1 system (ThermoFisher Scientific, Montigny-le-Bretonneux, France). Relative gene expression was determined as arbitrary unit as the ratio of target transcripts to reference genes, Acidic ribosomal phosphoprotein P0/ Ribosomal protein lateral stalk subunit P0 (*36B4/Rplp0*) and Hypoxanthine-guanine phosphoribosyltransferase (*Hprt*) in murine samples and, *RPLP0*, Glyceraldehyde-3-Phosphate Dehydrogenase (*GAPDH*) and Peptidylpropyl Isomerase A (*PPIA*) in human samples. All primer sequences are available in the Supplementary Table 2.

Protein extraction and analysis

Cultured cells, mouse liver and AT were solubilized as previously described (1). Equal protein amounts (20 µg) were separated by SDS-PAGE, transferred onto nitrocellulose membrane and immunodetected with antibodies (Supplementary Table 1). α -tubulin was used to normalize expression. The immunoreactive bands were revealed using the ECL detection kit (Pierce ECL Western Blotting substrate, Rockford, IL, USA) and analyzed using an iBright system (ThermoFisher, Montigny-le-Bretonneux, France). Ratio P-Akt/total-Akt was quantified using an ImageJ software (Chemi Genius2 scan, GeneSnap; Syngene, Cambridge, UK). VEGFA protein content was measured on adipose tissue extracts with the Quantikine ELISA mouse VEGF kit (R&D systems, Lille, France).

Chromatin Immunoprecipitation (ChIP)

Mature 3T3-F442A adipocytes treated with 100 nM dexamethasone under normoxic or hypoxic condition for 16 hours were homogenized using a mechanical disruption device (Lysing Matrix A, Fast Prep MP1, 3 × 40 sec, MP Biomedicals, Illkirch-Graffenstaden, France). Sonicated chromatin (15 µg) was isolated before chromatin immunoprecipitation and used as positive

control for the PCR experiments (input) as previously described in (2). Twenty μg of sonicated chromatin were incubated with 1 μg of rabbit polyclonal anti-HIF-1 α (ab1) antibody, or 10 μg of chicken anti-GFP antibody (a negative control), or 10 μg of rabbit polyclonal anti-histone H4 acetylated antibody (a positive control) for immunoprecipitation (Supplementary Table 1). The IP were performed using the ChIP assay kit (Upstate Biotechnology). The DNA was purified using the Nucleospin Gel and PCR Clean Up kit (Qiagen). ChIP products and inputs were then analyzed by quantitative SYBR-green real-time PCR, using primers described in the Supplementary Table 2. All cycle threshold (Ct) values were compared with the input amounts to normalize for variations and presented as fold-enrichment.

AT clearing and 3D-fluorescence imaging

After DyLight 649 labeled Lycopersicon Esculentum (Tomato) lectin or vehicle (as a negative control) injection, SCAT and GAT were collected and fixed in 4% paraformaldehyde (PFA) (pH=7) overnight at 4°C (Supplementary Table 1) and cleared as previously described (3). Briefly, AT were permeabilized, stained with Phalloidin-alexa488 and dehydrated in increasing bath of ethanol. AT were cleared in methyl-salicylate for at least 2 hours and imaged in an imaging chamber filled with methyl-salicylate using a Nikon A1R-confocal microscope equipped with a 20x long distance objective (C3M imaging facility, Nice, France). 3D stacks were acquired and a pipeline of image post-processing was applied using “bleach correction” and “Gaussian blur” imageJ plugins. 3D images were loaded in IMARIS software. Adipocytes were segmented by using phalloidin staining, vessels were segmented by using lectin staining, and the whole tissue volume were segmented using phalloidin staining. The volume of the vessels and of the whole tissue was obtained using IMARIS statistics. When noticed, these values were reported to the whole tissue volume estimated at sacrifice. Analysis and 3D Volume rendering movies were generated with IMARIS software. The specificity of the vessel staining

by lectin-DyLight 649 was verified in control mice receiving vehicle alone (Supplementary Fig. 1E). To determine the number of adipocytes per fat pad, we applied the mathematical estimation $N=M/(\rho \times (4/3 \pi R^3))$ as proposed by Jo *et al* (4): N represents the number of adipocytes, M the mass of adipose tissue, ρ the “probable density of adipocyte” (0.915 g/ml), and R the mean radius of adipocytes.

Patients with Cushing’s syndrome

Patients underwent unilateral adrenalectomy allowing, at the same time, biopsies of SCAT. Between 2010 and 2015, twenty patients were recruited by the Endocrinology Departments of the University Hospital centers of Saint-Antoine, Cochin, Pitié Salpêtrière (Paris), Bicêtre (Kremlin-Bicêtre), Henri Mondor (Créteil) and Haut-Lévêque (Bordeaux). Dual energy X-ray absorptiometry (DEXA) was performed to evaluate lean and fat mass body compositions at trunk, lower and upper limbs. Collection of clinical data and blood samples (5 mL) were carried out under appropriate conditions. Approximately 200 mg of SCAT was collected for each patient and stored in liquid nitrogen. SCAT and other metabolic parameters were compared between two subgroups of Cushing patients, determined according to the value of *VEGFA* expression, giving a "low *VEGFA* expressing" group and a "high *VEGFA* expressing" group. The clinical, biological and anthropometric data of Cushing patients are reported in Supplementary Tables 3 and 4.

Study approval

All experiments were carried out according to the European Communities Council Directive (2010/63/UE) for the care and use of animals for experimental procedures and complied with the regulations of the French Ethics Committee in Animal Experiment « Charles Darwin » (Ile-de-France, Paris, n°5). All procedures were approved by this committee (n° #4625-

2016032111413252v2 and 18442-201901141010547v1). For the human study, the LIPOCUSH cohort, whose National Clinical Trial (NCT) number is NCT01688349, was funded by an AP-HP Clinical Research Contract, and required the consent of all patients prior to participation.

References

1. Dalle H, Garcia M, Antoine B, Boehm V, Do T, Buyse M, Ledent T, Lamazière A, Magnan C, Postic C, Denis R, Luquet S, Fève B, Moldes M. Adipocyte Glucocorticoid Receptor Deficiency Promotes Adipose Tissue Expandability and Improves the Metabolic Profile Under Corticosterone Exposure. *Diabetes*. 2019;68: 305-317
2. Milet C, Bléher M, Allbright K, Orgeur M, Culpier F, Duprez D, Havis E. *Egr1* deficiency induces browning of inguinal subcutaneous white adipose tissue in mice. *Sci Rep*. 2017;7: 16153
3. Gilleron J, Meziat C, Sulen A, Ivanov S, Jager J, Estève D, Muller C, Tanti J, Cormont M. Exploring Adipose Tissue Structure by Methylsalicylate Clearing and 3D Imaging. *J Vis Exp*. 2020;162
4. Jo J, Gavrilova O, Pack S, Jou W, Mullen S, Sumner A, Cushman S, Periwai V. Hypertrophy and/or Hyperplasia: Dynamics of Adipose Tissue Growth. *PLoS Comput Biol*. 2009;5: e1000324

Supplementary Table 1: List of antibodies

| Experiment | Antibodies | Reference | Company | Dilution or concentration |
|--------------------------------|--|---------------|--|---------------------------|
| IHC | Monoclonal anti-CD31 | # sc-53411 | Santa Cruz Biotechnology, Germany | 1:50 |
| | Normal mouse IgG1 | # sc-3877 | Santa Cruz Biotechnology, Germany | 1:50 |
| | Secondary antibody biotinylated | # RPN 1001 | Amersham, Les Ulis, France | 1:5000 |
| | Streptavidine-HRP | # 016-030-084 | Jackson Immuno Research, Cambridgeshire, UK | 1:100 |
| FACS | Alexa-Fluor® 488 anti-mouse CD45 | #160306 | BioLegend, London, UK | 1.25 µg/µl |
| | Alexa-Fluor® 488 rat IgG2a, κ isotype control | #400525 | BioLegend, London, UK | 1.25 µg/µl |
| | Brilliant Violet™ 421 anti-mouse CD31 | #102424 | BioLegend, London, UK | 1.25 µg/µl |
| | Brilliant Violet™ 421 rat IgG2a, κ isotype control | #400549 | BioLegend, London, UK | 1.25 µg/µl |
| 3D fluorescence imaging | DyLight 649 Lycopersicon Esculentum Lectin | #DL-1178-1 | Vector Laboratories Burlingame, USA | 2 µg/µl |
| WB | Rabbit polyclonal anti-Phospho-Akt (Ser 473) | # 9271L | Cell Signaling Technology, Danvers, MA, USA | 1:1000 |
| | Rabbit polyclonal anti-Akt | # 9272S | Cell Signaling Technology, Danvers, MA, USA | 1:1000 |
| | Rabbit polyclonal anti-HIF-1α | # NB100-449 | Bio-Techne Ltd., Abingdon, UK | 1:500 |
| | Monoclonal anti α-tubulin | #T5168 | Sigma-Aldrich, Saint Quentin Fallavier, France | 1:10,000 |
| | Anti-rabbit IgG HRP-linked | #7074S | Cell Signaling Technology, Danvers, MA, USA | 1:5000 |
| | Anti-mouse IgG HRP-linked | #7076S | Cell Signaling Technology, Danvers, MA, USA | 1:5000 |
| ChIP | Rabbit polyclonal anti-HIF-1α | # NB100-449 | Bio-Techne Ltd., Abingdon, UK | 1:200 |
| | Chicken polyclonal anti-GFP | # GFP 1020 | Interchim, Montluçon France | 1:1000 |
| | Rabbit polyclonal anti-Histone H4a | # 06-866 | Sigma-Aldrich, France | 1:100 |

Supplementary Table 2: List of murine and human primers for RT-qPCR and ChIP analysis

| Gene | Forward primers | Reverse primers |
|---|--------------------------------|------------------------------------|
| <i>Mouse 36b4</i> | 5'-GCTGATGGGCAAGAACACCA-3' | 5'-CCCAAAGCCTGGAAGAAGGA-3' |
| <i>Mouse Hpvt</i> | 5'-AGGACCTCTCGAAGTGT-3' | 5'-TCAAATCCCTGAAGTACTCAT-3' |
| <i>Mouse Gr</i> | 5'-GGGCGCCAAGTGATTGCCGCAGT-3' | 5'-CCAACCCAGGGCAAATGCCATGA-3' |
| <i>Mouse Fkbp5</i> | 5'-TGTTCAAGAAGTTCGCAGAGC-3' | 5'-CCTTCTTGCTCCCAGCTTT-3' |
| <i>Mouse Vegfa</i> | 5'-AAAAACGAAAGCGCAAGAAA-3' | 5'-TTTCTCCGCTCTGAACAAAGG-3' |
| <i>Mouse Hif-1α</i> | 5'-GCACTAGACAAAGTTCACCTGAGA-3' | 5'-CGCTATCCACATCAAAGCAA-3' |
| <i>Mouse Slc2a1</i> | 5'-CCACAGTGAAGGCCGTGTT-3' | 5'-GGTATCAATGCTGTGTTCTACTACTACA-3' |
| <i>Mouse Esm1</i> | 5'-CAGTATGCAGCAGCCAAATC-3' | 5'-GATGCTGAGTCACGCTCTGT-3' |
| <i>HRE-containing murine Vegfa promoter</i> | 5'-CGAGGGTTGGCGGCAGGAC-3' | 5'-CAGTGGCGGGGAGTGAGACG-3' |
| <i>Human RPLP0</i> | 5'-GGCGACCTGGAAGTCCAAC-3' | 5'-CCATCAGCACCACAGCCTTC-3' |
| <i>Human GAPDH</i> | 5'-AGCCACATCGCTCAGACAC-3' | 5'-GCCCAATACGACCAAATCC-3' |
| <i>Human PPIA</i> | 5'-ATGCTGGACCCAACACAAAT-3' | 5'-TCTTTCACTTTGCCAAACACC-3' |
| <i>Human VEGFA</i> | 5'-TGCCGCCACACCATCAC-3' | 5'-GTCTCGCCCTCCGGACCCAA-3' |
| <i>Human NR3C1</i> | 5'-CCTTCTGCGTTCACAAGCTA-3' | 5'-TTCTTTGGAGTCCATCAGTGAAT-3' |
| <i>Human HSD1B11</i> | 5'-TCTGTGTTCTTGGCCTCATAGA-3' | 5'-GAGCTGCTTGCATATGGACTATC-3' |
| <i>Human C/EBPB</i> | 5'-TGCTTGAACAAGTTGGGCAG-3' | 5'-GCGCGAGCGCAACAACA-3' |
| <i>Human C/EBPD</i> | 5'-GGACATAGGAGCGCAAAGAA -3' | 5'-GCTTCTCTCGCAGTTTAGTGG-3' |
| <i>Human C/EBPA</i> | 5'-GACATCAGCGCCTACATCG-3' | 5'-GGCTGTGCTGGAACAGGT-3' |
| <i>Human PPARG</i> | 5'-CTCATATCCGAGGGCCAA-3' | 5'-TGCCAAGTCGCTGTCATC-3' |
| <i>Human SREBF1C</i> | 5'-GGAGGGGTAGGCCAACGGCCT-3' | 5'-CATGTCTTCGAAAGTGCAATCC-3' |
| <i>Human FASN</i> | 5'-CAGGCACACACGATGGAC-3' | 5'-CGGAGTGAATCTGGGTTGAT-3' |
| <i>Human Leptin</i> | 5'-TTGTCACCAGGATCAATGACA-3' | 5'-GTCCAAACCGGTGACTTTCT-3' |
| <i>Human Adiponectin</i> | 5'-GGTGAGAAGGGTGAGAAAGGA-3' | 5'-TTTCACCGATGTCTCCCTTAG-3' |

Supplementary Table 3. Relationship between *VEGFA* gene expression and clinical and biological parameters of patients with Cushing's syndrome

Twenty patients with a Cushing's syndrome related to a cortisolic adenoma (LIPOCUSH cohort) were divided in two subgroups according to their lowest and highest levels of *VEGFA* expression in SCAT, based on the stratified median of *VEGFA* gene expression (10 per group, unless indicated). Data are presented as the mean \pm SD. * $P < 0.05$, as determined by Student's t Welch and Mann-Whitney tests to compare means. (HOMA-IR: homeostatic model assessment of insulin resistance, HbA1c: glycated hemoglobin A1c, TG: triglycerides, FFA: free fatty acids)

| Biological parameters | All patients with Cushing's syndrome | Patients with the lowest <i>VEGFA</i> expression in SCAT | Patients with the highest <i>VEGFA</i> expression in SCAT | <i>P</i> -value |
|---|--------------------------------------|--|---|------------------|
| Total number | 20 | 10 | 10 | - |
| Gender (M/F) | 2/18 | 1/9 | 1/9 | - |
| Age (years) (<i>n</i> =20) | 46.4 \pm 14.2 | 50.3 \pm 12.2 | 42.5 \pm 15.5 | <i>P</i> =0.228 |
| Midnight cortisol levels (μ g/dL) (<i>n</i> =15) | 19 \pm 12.7 | 19.9 \pm 17.4 | 18.2 \pm 7.8 | <i>P</i> =0.444 |
| Serum cortisol levels after 1 mg Dex (μ g/dL) (<i>n</i> =15) | 18 \pm 11 | 15.7 \pm 12.2 | 20.7 \pm 9.5 | <i>P</i> =0.394 |
| Free urinary Cortisol (nmol/24h) (<i>n</i> =18) | 423.7 \pm 442 | 293.1 \pm 261.2 | 587 \pm 576 | <i>P</i> =0.360 |
| HOMA-IR (<i>n</i> =15) | 3.1 \pm 4.3 | 5.3 \pm 5.9 | 1.3 \pm 0.8 | <i>P</i> =0.029* |
| HbA1c (%) (<i>n</i> =16) | 6.5 \pm 1.5 | 7.1 \pm 1.7 | 5.7 \pm 0.6 | <i>P</i> =0.037* |
| TG (mmol/L) (<i>n</i> =14) | 2.2 \pm 2.0 | 2.1 \pm 1.5 | 2.4 \pm 2.6 | <i>P</i> =0.950 |
| FFA (mmol/L) (<i>n</i> =20) | 0.62 \pm 0.20 | 0.64 \pm 0.23 | 0.62 \pm 0.19 | <i>P</i> =0.837 |

Supplementary Table 4. Relationship between *VEGFA* gene expression and anthropometric parameters of patients with Cushing's syndrome

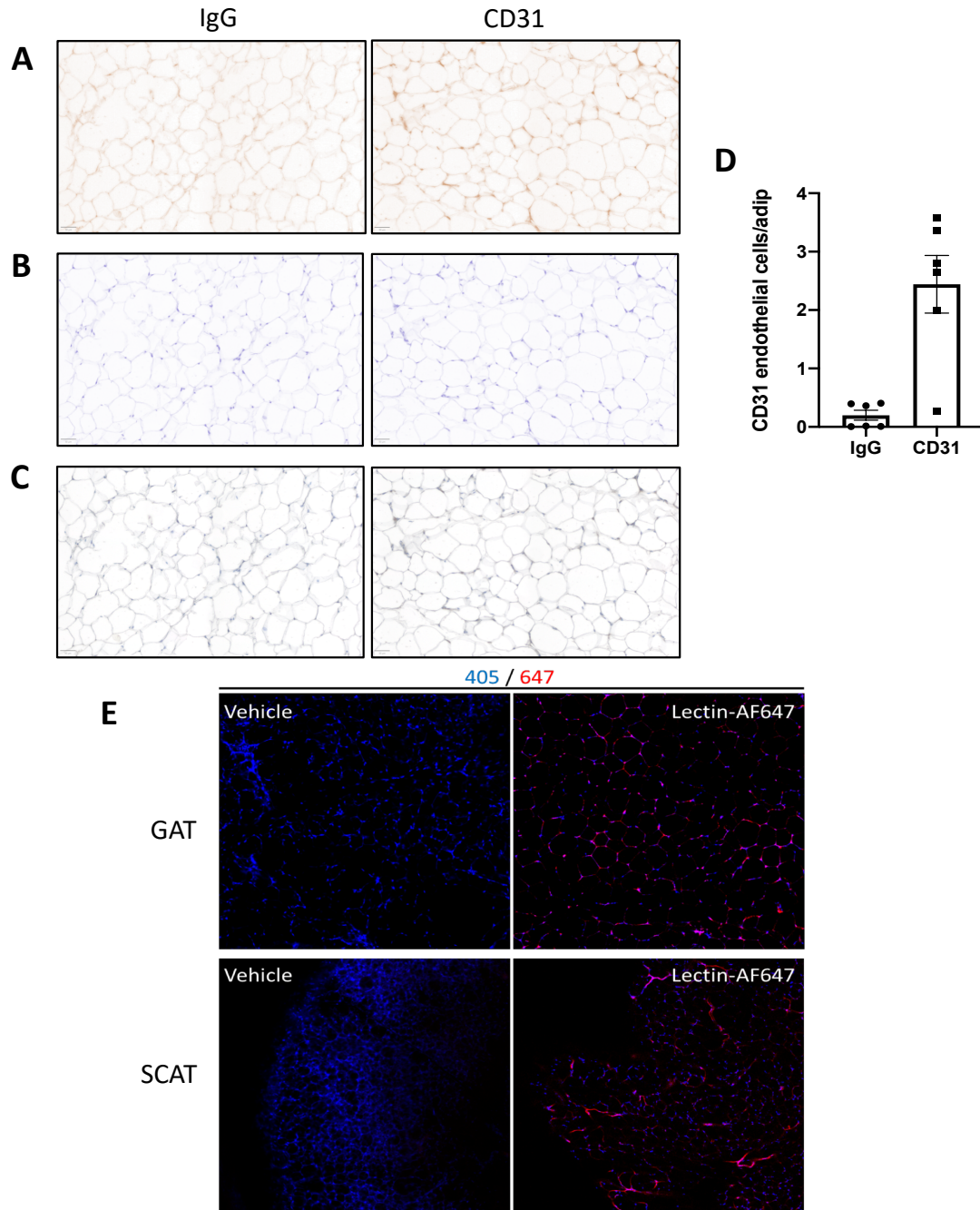
Eleven patients of the LIPOCUSH cohort underwent DEXA analysis to determine body fat repartition. We divided them into two subgroups according to their lowest (n = 4) and highest (n = 7) levels of *VEGFA* expression as in Supplementary Table 3. Data are presented as the mean \pm SD. *P<0.05, as determined by Student's t Welch and Mann-Whitney tests to compare means.

| Anthropometric parameters | All patients with Cushing's syndrome | Patients with the lowest <i>VEGFA</i> expression in SCAT | Patients with the highest <i>VEGFA</i> expression in SCAT | P-value |
|--|--------------------------------------|--|---|------------------|
| BMI (kg/m ²) | 30.0 \pm 7.7 | 36.2 \pm 9.3 | 26.4 \pm 3.9 | <i>P</i> =0.123 |
| Total fat mass (kg) | 38.9 \pm 15.4 | 44.1 \pm 17.5 | 36.0 \pm 15.0 | <i>P</i> =0.465 |
| Total fat mass (% of total body mass) | 43.4 \pm 9.2 | 42.4 \pm 11.9 | 43.9 \pm 8.4 | <i>P</i> =0.827 |
| Upper limb fat mass (% of upper limb mass) | 23.7 \pm 16.4 | 12.7 \pm 4.6 | 29.9 \pm 17.6 | <i>P</i> =0.043* |
| Lower limb fat mass (% of lower limb mass) | 36.2 \pm 12.7 | 26.7 \pm 5 | 41.6 \pm 12.8 | <i>P</i> =0.021* |
| Trunk fat mass (% of trunk mass) | 48.9 \pm 9.9 | 50.7 \pm 13.3 | 47.9 \pm 8.4 | <i>P</i> =0.726 |

Supplementary Table 5. Correlation between *VEGFA* expression and clinical, anthropometric and molecular traits of patients with Cushing's syndrome

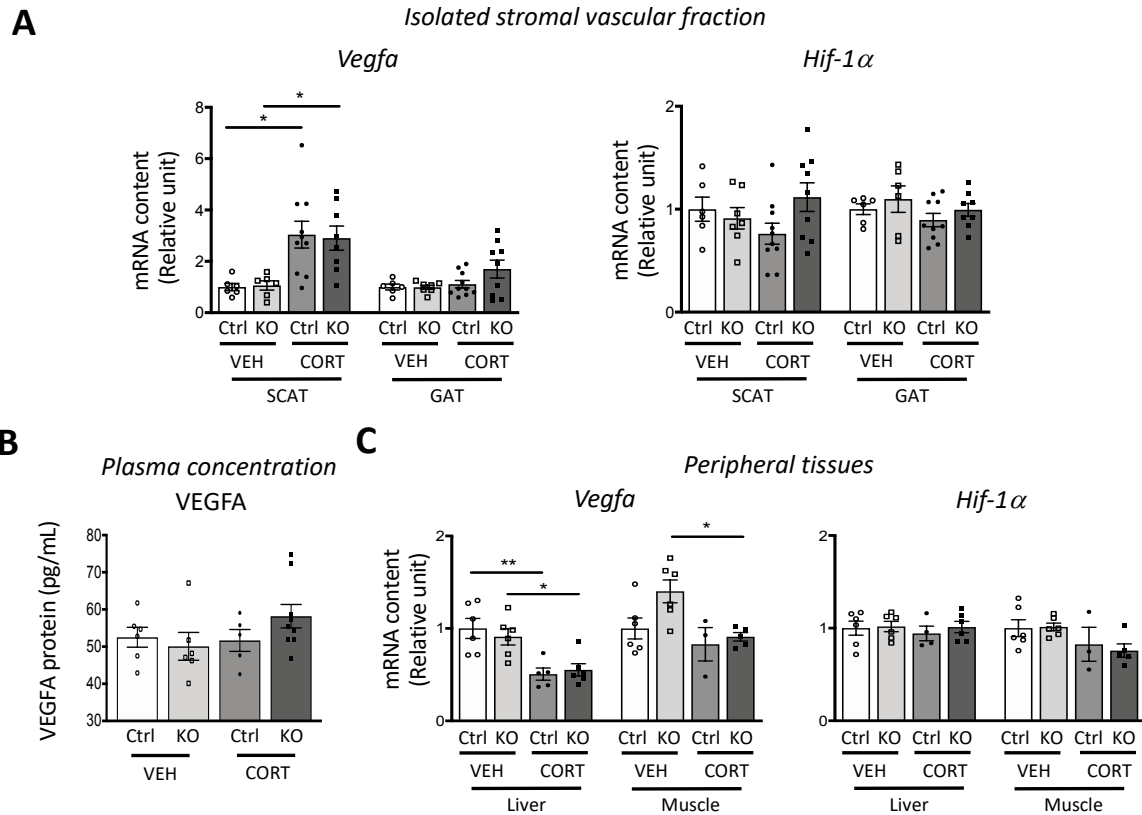
Correlations (Spearman's test) were performed between *VEGFA* expression and clinical, anthropometric parameters (n=11-15), and adipocyte-related gene expression in SCAT (determined by RT-PCR; n=20) from patients with Cushing's syndrome (LIPOCUSH cohort). (HOMA-IR: homeostatic model assessment of insulin resistance, BMI: body mass index).

| | | <i>VEGFA</i> | |
|-------------------------------------|---------------------|--------------|----------|
| | | <i>r</i> | <i>P</i> |
| Clinical parameter | HOMA-IR | -0.494 | 0.054 |
| Anthropometric parameters | BMI | -0.527 | 0.017 |
| | Trunk fat mass | -0.409 | 0.214 |
| | Upper limb fat mass | 0.715 | 0.016 |
| | Lower limb fat mass | 0.691 | 0.023 |
| GC signaling pathway markers | <i>NR3C1</i> | 0.777 | 5.49E-05 |
| | <i>HSB11B1</i> | -0.451 | 0.046 |
| Adipogenic markers | <i>C/EBPB</i> | 0.580 | 0.007 |
| | <i>C/EBPD</i> | 0.683 | 0.001 |
| | <i>PPARG</i> | 0.571 | 0.008 |
| | <i>C/EBPA</i> | 0.517 | 0.020 |
| Lipogenic markers | <i>SREBF1</i> | 0.624 | 0.003 |
| | <i>FASN</i> | 0.792 | 3.10E-05 |
| Adipokine | <i>ADIPOQ</i> | 0.785 | 4.15E-05 |



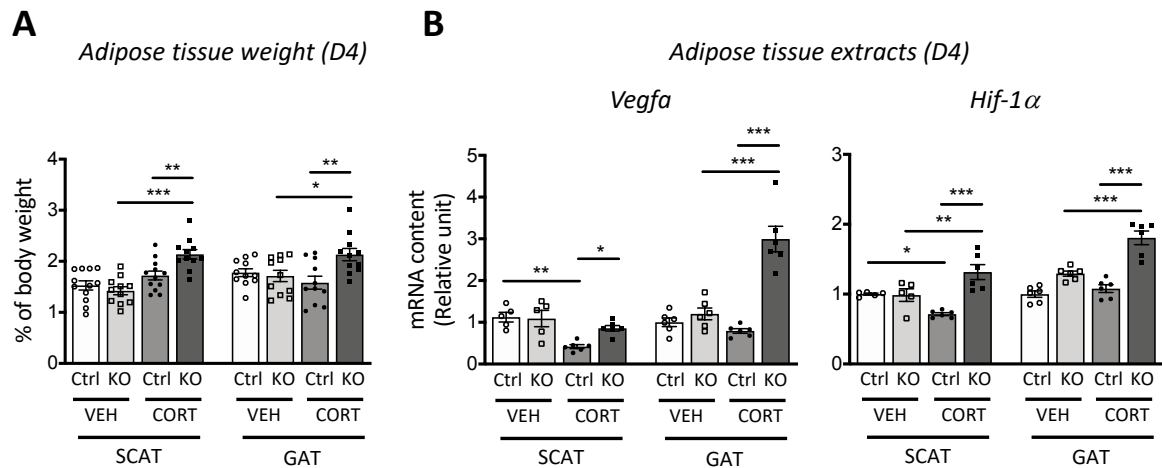
Supplementary Figure 1. Negative controls for histology and cleared adipose tissue from AdipoGR-KO and control mice. Related to Fig. 3 and to Fig. 4.

The specificity of the CD31 histologic staining was verified on subcutaneous adipose tissue (SCAT) sections from CORT-treated AdipoGR-KO mice (A-D). The specificity of the lectin fluorescence was analyzed on cleared adipose tissue from control mice (E). A-C: SCAT sections were stained with either a non-relevant IgG1 antibody (left panels) or a specific anti-CD31 antibody (right panels). DAB staining is shown in (A), H&E staining in (B) and the merged images in (C). D: Quantification of labeled endothelial cells per adipocyte. E: Non-specific fluorescence in the far-red wavelength was determined on cleared subcutaneous (SCAT) and gonadal (GAT) adipose tissues from control mice IV-injected with either lectin-DyLight 649 or vehicle alone. Cell nuclei were stained with Dapi. The images presented here are issued from a single confocal plan view.



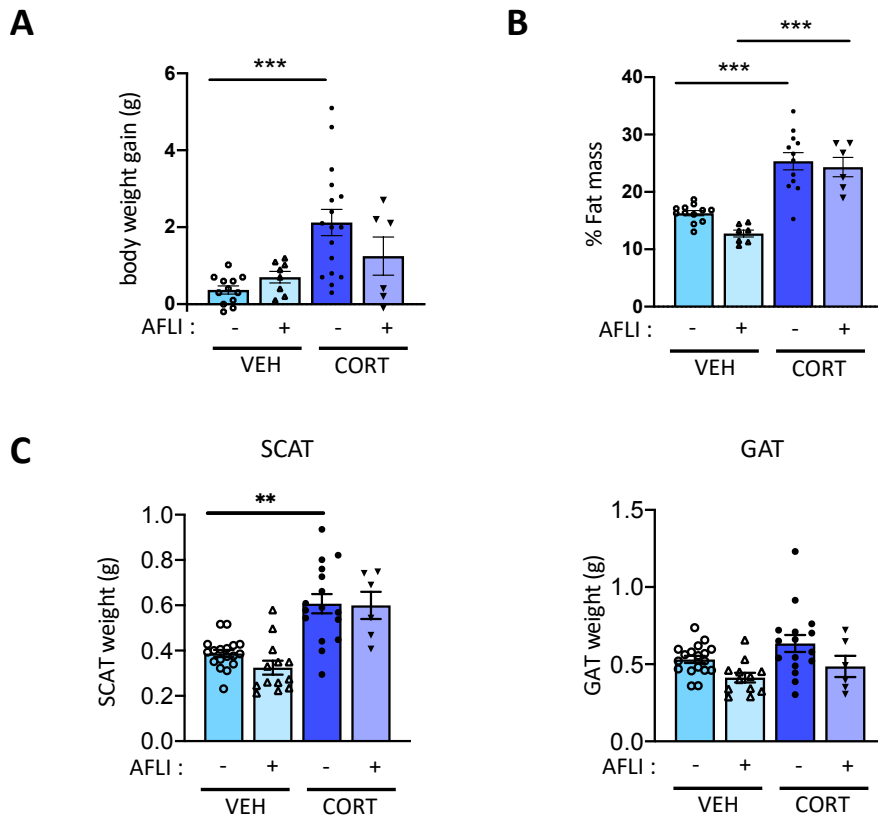
Supplementary Figure 2. Expression of Vegfa and Hif-1 α in adipocyte-specific Gr-deficient mice treated with VEH or CORT. Related to Fig. 1.

Control (Ctrl) and AdipoGR-KO mice were analyzed after 4 weeks of exposure with VEH or CORT. A: Relative gene expression was determined by RT-qPCR for Vegfa and Hif-1 α mRNA content in the stromal vascular fraction ($n = 6-10/\text{group}$) isolated from SCAT and GAT. B: VEGFA protein concentration was measured in plasma samples of VEH- and CORT-treated Ctrl and AdipoGR-KO mice ($n = 5-9/\text{group}$). C: Vegfa and Hif-1 α mRNA expression was determined by RT-qPCR in the liver and muscle of mice ($n = 3-6/\text{group}$). Data are presented as the mean \pm SEM. Each data point represents one animal. * $P < 0.05$, ** $P < 0.01$, as determined by one-way ANOVA, followed by the Bonferroni post-hoc test to compare means.



Supplementary Figure 3. AdipoGR-KO mice display an enhanced body weight and expression of *Vegfa* and *Hif-1α* from 4 days of CORT treatment. Related to Fig. 1

Control (Ctrl) and AdipoGR-KO mice were analyzed at day 4 (D4) of VEH or CORT treatment. A: Subcutaneous adipose tissue (SCAT) and gonadal adipose tissue (GAT) weights are presented as the percentage of total body weight of Ctrl and AdipoGR-KO mice ($n = 11-12/\text{group}$). B: Relative gene expression of *Vegfa* and *Hif-1α* was determined by RT-qPCR in SCAT and GAT ($n = 5-6/\text{group}$). Data are presented as the mean \pm SEM. Each data point represents one animal. * $P < 0.05$, ** $P < 0.01$ and *** $P < 0.001$, as determined by one-way ANOVA, followed by the Bonferroni post-hoc test to compare means.



Supplementary Figure 4. Effect of Aflibercept treatment on VEH- and CORT-treated control mice.

Related to Fig. 4.

Control (Ctrl) mice were treated with VEH or CORT alone, or in combination with the soluble decoy receptor, Aflibercept (AFLI) or the vehicle solution (PBS) during 4 weeks. A: Body weight gain is presented after 4 weeks of treatment (n = 6-17/group). B: Fat body mass was determined by DEXA analyzer (n = 6-12/group). C: SCAT and GAT weights of Ctrl mice were presented in grams (n = 5-18/group). Data are presented as the mean \pm SEM. Each data point represents one animal. ** $P < 0.01$ and *** $P < 0.001$ as determined by one-way ANOVA, followed by the Bonferroni post-hoc test to compare means.

Supplemental Movies

Supplementary Movie 1. SCAT vascular network of VEH-treated control mice

Supplementary Movie 2. SCAT vascular network of VEH-treated AdipoGR-KO mice

Supplementary Movie 3. SCAT vascular network of CORT-treated control mice

Supplementary Movie 4. SCAT vascular network of CORT-treated AdipoGR-KO mice

Supplementary Movie 5. GAT vascular network of VEH-treated control mice

Supplementary Movie 6. GAT vascular network of VEH-treated AdipoGR-KO mice

Supplementary Movie 7. GAT vascular network of CORT-treated control mice

Supplementary Movie 8. GAT vascular network of CORT-treated AdipoGR-KO mice